Optical near-field mapping of excitons and biexcitons in naturally occurring semiconductor quantum dots

Ulrich Hohenester*
Institut für Theoretische Physik, Karl–Franzens–Universität Graz, Universitätsplatz 5, 8010 Graz, Austria

Guido Goldoni and Elisa Molinari
INFM–S^3 and Dipartimento di Fisica, Università di Modena e Reggio Emilia, Via Campi 213/A, 41100 Modena, Italy
(Dated: April 1, 2004)

We calculate the near-field optical spectra of excitons and biexcitons in semiconductor quantum dots naturally occurring at interface fluctuations in GaAs-based quantum wells, using a non-local description of the response function to a spatially modulated electro-magnetic field. The relative intensity of the lowest, far-field forbidden excitonic states is predicted; the spatial extension of the ground biexciton state is found in agreement with recently published experiments.

Optical manipulation of states in quantum dots (QDs) is a key towards the implementation of quantum information processing in semiconductors.[1–3] Important features of QDs are not only that excitations are fully discrete in energy resulting in long coherence times,[4,5] but also that they are governed by the Coulomb interaction between electrons and holes which gives rise to specific few-particle aggregates as a result of photoexcitation. Based on this unique mechanism, all-optical conditional control of exciton and biexciton states were proposed and demonstrated for quantum computing schemes in QD structures.[2,6]

The use of local probes for a detailed understanding of these interacting states and their real-space distribution is thus of great interest for their engineering, and might open the way to the important goal of direct optical manipulation of individual states in coupled structures. The so-called natural QDs —or terraces—, where quantum confinement is induced by local monolayer fluctuations in the thickness of a semiconductor quantum well, have sofar been excellent laboratories for the study of these novel phenomena because quantization is combined with a large oscillator strength associated to the large active volume of the QD.[7] The huge progress in probe preparation has lead to resolutions which in this class of systems have reached the scale of the constituent quantum states.[8–11]

In this letter, we investigate theoretically the optical response of excitons and biexcitons in natural QDs in near-field experiments. We calculate the spatial maps of the exciton and biexciton low-energy states, taking into account the non-local susceptibility of the electromagnetic (EM) field, and show that the spatial extension depends on the correlated state, being narrower for biexcitons, in agreement with experimental findings. We also calculate the oscillator strengths of the lowest, far-field forbidden excitonic states, and show that they can be comparable to the ground state, thus allowing for their observation at the presently achievable resolution scale.

Exciton and biexciton states. For excitonic complexes bound to interface fluctuations, where the confinement considerably exceeds the excitonic Bohr radius, center-of-mass and relative motion of the electron-hole pairs can be decoupled. Then, the in-plane part of the exciton and biexciton wavefunctions, Ψ^x and $\bar{\Psi}^b$, respectively, can be approximately written as[12]

$$\begin{aligned} \Psi^x(\boldsymbol{r}_1,\boldsymbol{r}_a) &\cong \phi_o(\boldsymbol{r}_1,\boldsymbol{r}_a)\,\Phi^x(\boldsymbol{R}_x) \\ \bar{\Psi}^b(\boldsymbol{r}_1,\boldsymbol{r}_2,\boldsymbol{r}_a,\boldsymbol{r}_b) &\cong \bar{\phi}_o(\boldsymbol{r}_1,\boldsymbol{r}_2,\boldsymbol{r}_a,\boldsymbol{r}_b)\,\bar{\Phi}^b(\boldsymbol{R}_b)\,. \end{aligned} \quad (1)$$

Here, ϕ_o and $\bar{\phi}_o$ are the exciton and biexciton wavefunctions for an ideal quantum well, whereas Φ^x and $\bar{\Phi}^b$ are the envelope functions accounting for interface fluctuations. We denote electrons with $\boldsymbol{r}_1$ and $\boldsymbol{r}_2$, holes with $\boldsymbol{r}_a$ and $\boldsymbol{r}_b$, and finally the exciton and biexciton center-of-mass coordinates with $\boldsymbol{R}_x$ and $\boldsymbol{R}_b$. The specific forms of ϕ_o and $\bar{\phi}_o$ are taken from Kleinman[13] for a 5 nm

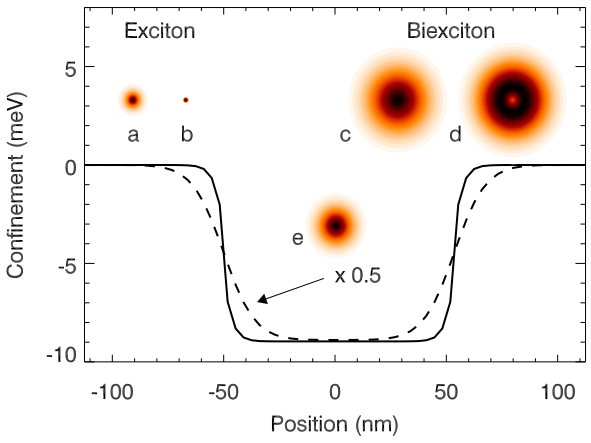

FIG. 1: Confinement potential along x for the center-of-mass motion of excitons (solid line) and biexcitons (dashed line).[21] The insets report the exciton probability distributions $p_i(\boldsymbol{r})$ for (a) electrons and (b) holes, the biexciton probability distributions $\bar{p}_i(\boldsymbol{r})$ for (c) electrons and (d) holes, and (e) $\mu(\boldsymbol{r})$ the probability of creating a second electron-hole pair at distance $\boldsymbol{r}$ from the exciton center of mass. The reduced probability at the center of (d) is attributed to the repulsive part χ of the trial wavefunction.[13]

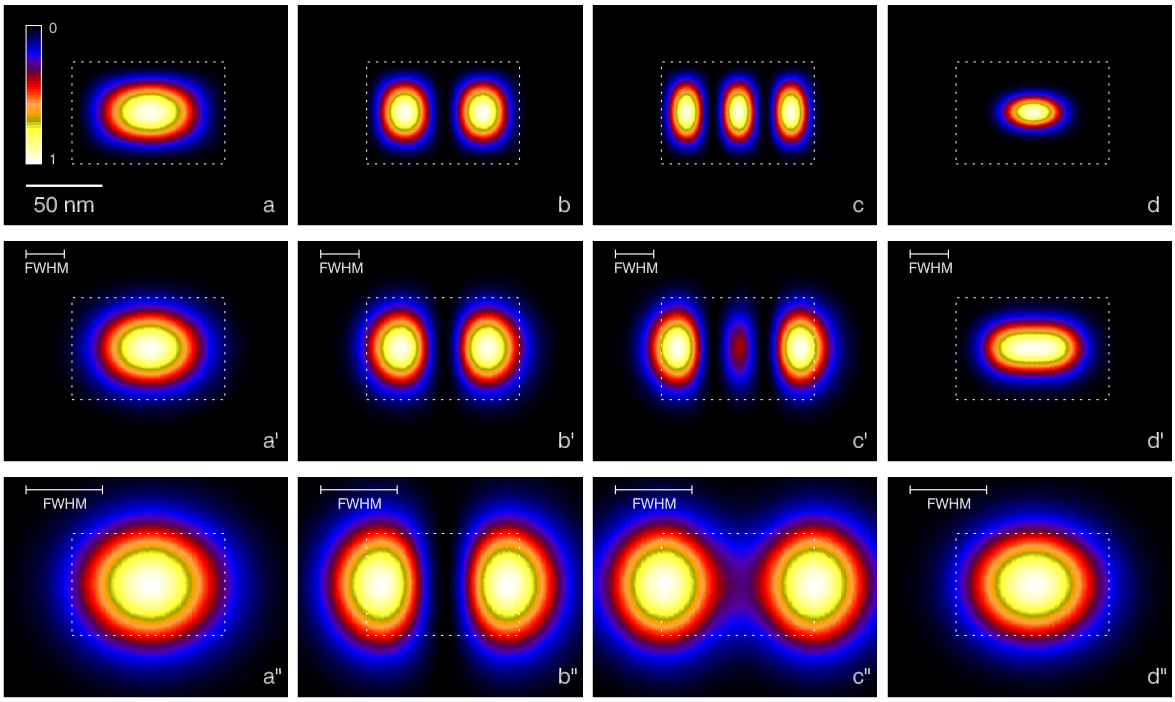

FIG. 2: (a–d) Real-space map of the square modulus of the wavefunctions for the exciton (a) ground state, (b) first and (c) third excited state, and (d) the biexciton ground state;[21] the dashed lines indicate the boundaries of the assumed interface fluctuation. (a'–d') Near-field spectra for a spatial resolution of 25 nm and (a"–d") 50 nm, as computed according to Refs. 17,18 and eq. (3). The FWHM of the assumed EM-field distribution is indicated in the 2nd and 3rd row

thick quantum well, i.e., the usual two-dimensional exciton state $\propto \exp -kr_{1a}$, $k = 1.94$ in units of the Bohr radius a_o, and the biexciton state $\psi(r_{1a}, r_{1b}, r_{2a}, r_{2b})\chi(r_{ab})$, which consists of trial wavefunctions ψ and χ associated to the attractive electron-hole[14] and repulsive hole-hole[15] interactions, respectively; r_{ij} is the distance between particles i and j.

We consider a prototypical interface-fluctuation confinement of rectangular shape with dimensions 100×70 nm^2, and monolayer fluctuations of a 5 nm thick well.[10,11] The exciton confinement is then given by the well-width dependent electron and hole single-particle energies along z convoluted with the probabilities $p_i(\boldsymbol{r} - \boldsymbol{R})$ of finding an electron or hole at distance $\boldsymbol{r}$ from the center-of-mass coordinate $\boldsymbol{R}$,[12] with a straightforward generalization to biexcitons ($\boldsymbol{\tau}$ and $\bar{\boldsymbol{\tau}}$ denote the phase space for excitons and biexcitons, respectively)

$$\begin{aligned} p_i(\boldsymbol{r} - \boldsymbol{R}) &= \int d\boldsymbol{\tau}\, \delta(\boldsymbol{R} - \boldsymbol{R}_x)\delta(\boldsymbol{r} - \boldsymbol{r}_i)\, \phi_o^2(\boldsymbol{r}_1, \boldsymbol{r}_a) \\ \bar{p}_i(\boldsymbol{r} - \boldsymbol{R}) &= \int d\bar{\boldsymbol{\tau}}\, \delta(\boldsymbol{R} - \boldsymbol{R}_b)\delta(\boldsymbol{r} - \boldsymbol{r}_i)\, \bar{\phi}_o^2(\boldsymbol{r}_1, \boldsymbol{r}_2, \boldsymbol{r}_a, \boldsymbol{r}_b)\,. \end{aligned} \tag{2}$$

Figure 1 shows the effective confinement potential for excitons (solid line) and biexcitons (dashed line). The insets show that for excitons the electron probability distribution $p_e(\boldsymbol{r})$ extends over the effective Bohr radius $k^{-1}a_o$ whereas $p_h(\boldsymbol{r})$ is strongly peaked around $\boldsymbol{0}$; in contrast, for the biexcitons the weaker Coulomb binding results in a strong delocalization of the two-exciton complex.[13] As consequence, the biexciton center-of-mass motion is confined within a significantly smaller region.

The resulting two-dimensional Schrödinger equation for the exciton and biexciton center-of-mass wavefunctions $\Phi^x(\boldsymbol{R}_x)$ and $\bar{\Phi}^b(\boldsymbol{R}_b)$, respectively, are solved through a real-space discretization and numerical diagonalization on a grid of typical dimensions 64×64, similarly to the procedure described in Ref. 16. The computed exciton and biexciton states exhibit symmetries reminiscent of the two-dimensional box-like confinement,[21] i.e., an s-like exciton groundstate (fig. 2a), two p-like excited states of lowest energy with nodes along x (fig. 2b) and y (not shown), and two nodes along x for the third excited exciton state (fig. 2c); finally, the biexciton groundstate (fig. 2d) indeed shows a much stronger localization than the exciton groundstate (fig. 2a).

Near-field spectra. When the EM-field is modulated on the scale of the relevant quantum states, the non-local response of the system must be taken into account.[17] In addition to the relaxation of the far-field selection rules due to the different symmetry of the field with respect to the quantum states, spatial coherence may give rise to interference effects, so that collected spatial maps may be non-trivially related to the localization of the excitonic wavefunctions. We compute the near-field spectra

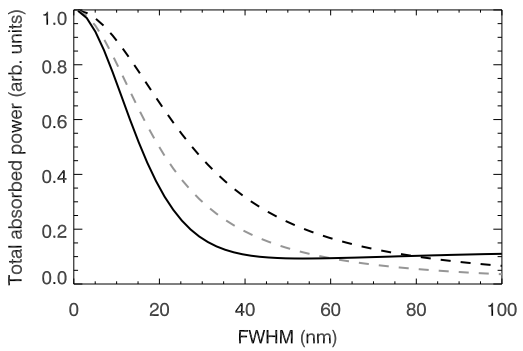

FIG. 3: Total absorbed power of the first (black, dashed line), second (gray, dashed line), and third (black, solid line) excited exciton state as a function of the spatial resolution of ξ. For all resolutions the spectra are normalized to the ground state absorption. The first and second excited excitons are far-field forbidden, whereas the oscillator strengths of the third excited state is approximately one ninth of that of the ground state.

analogously to the procedure described in Refs. 17,18 for an EM-field distribution $\xi(\boldsymbol{R}_{\rm tip}-\boldsymbol{r})$ of Gaussian shape centered around the tip position $\boldsymbol{R}_{\rm tip}$. For the excitons the local absorption spectra at a given exciton energy E_x are then given by the square modulus of the convolution of ξ with the exciton wavefunction Φ^x.[16,18] For the biexciton we have to be more specific of how the system is excited. We shall assume that the QD is initially populated by the ground state exciton and that the near-field tip probes the transition to the biexciton states. This situation approximately corresponds to that of Refs. 10,11 with non-resonant excitation in the nonlinear power regime. The local spectra are then proportional to[19] $\int d\boldsymbol{r}\, \xi(\boldsymbol{R}_{\rm tip}-\boldsymbol{r})\langle x|\hat{\psi}_h(\boldsymbol{r})\hat{\psi}_e(\boldsymbol{r})|b\rangle$, with x and b denoting the exciton and biexciton states of eq. (1), respectively, and $\hat{\psi}_{e(h)}(\boldsymbol{r})$ is the usual fermionic field operator for electrons (holes). Then, the square modulus of

$$\int d\boldsymbol{R}\, \Phi^x(\boldsymbol{R})\, \mu(\boldsymbol{r}-\boldsymbol{R})\, \bar{\Phi}^b(\frac{\boldsymbol{r}+\boldsymbol{R}}{2}) \qquad (3)$$

convoluted with ξ gives the optical near-field spectra corresponding to the transition from x to b, with $\mu(\boldsymbol{r}-\boldsymbol{R}) = \int d\boldsymbol{\tau}\, \delta(\boldsymbol{R}-\boldsymbol{R}_x)\, \phi_o(\boldsymbol{r}_1,\boldsymbol{r}_a)\bar{\phi}_o(\boldsymbol{r},\boldsymbol{r}_1,\boldsymbol{r},\boldsymbol{r}_a)$ giving the probability of exciting an electron-hole pair at $\boldsymbol{r}$ when an exciton is located at $\boldsymbol{R}$ (see fig. 1e)[19].

In the second and third rows of fig. 2 we report our calculated optical near-field spectra for spatial resolutions of 25 and 50 nm. It should be noted that the first (fig. 2b) and second excited state (not shown) are dipole forbidden, but have large oscillator strengths for both resolutions. Note also that, as a result of interference effects, the spatial maps at finite spatial resolutions differ somewhat from the wavefunction maps, particularly for the excited states: the apparent localization is weaker and, in (c), the central lobe is very weak for both resolutions. Finally, we observe that for the smaller spatial resolution the biexciton ground state depicts a stronger degree of localization than the exciton one, in nice agreement with the recent experiment of Matsuda et al.[10,11].

In order to be more quantitative and show if near-field experiments may distinguish the dipole forbidden transitions, we have calculated the total absorbed power (i.e., the incoherently summed intensity of the maps exemplified in fig. 2) as a function of the spatial resolution. Figure 3 shows that the intensity of the lowest dipole-forbidden state is a substantial fraction of the ground state intensity, and larger than the next dipole allowed excited states up to resolutions comparable with the QD linear dimensions. Indeed, preliminary results indicate that p-like structures have been seen in the sample of Ref. 9.[20]

We thank K. Matsuda for helpful discussions. This work has been supported in part by the EU under the TMR network "Exciting", the Austrian science fund FWF under project P15752–N08, the Italian Minister for University and Research under project FIRB *Quantum phases of ultra-low electron density semiconductor heterostructures*, and by INFM I.T. Calcolo Parallelo (2003).

* Electronic address: ulrich.hohenester@uni-graz.at

[1] A. Barenco, D. Deutsch, A. Ekert, and R. Josza, Phys. Rev. Lett. **74**, 4083 (1995).
[2] F. Troiani, U. Hohenester, and E. Molinari, Phys. Rev. B **62**, 2263 (2000).
[3] E. Biolatti, R. Iotti, P. Zanardi, and F. Rossi, Phys. Rev. Lett. **85**, 5647 (2000).
[4] N. H. Bondaeo, J. Erland, D. Gammon, D. Park, D. S. Katzer, and D. G. Steel, Science **282**, 1473 (1998).
[5] A. Zrenner, J. Chem. Phys. **112**, 7790 (2000).
[6] X. Li *et al.*, Science **301**, 809 (2003).
[7] G. Bastard, *Wave Mechanics Applied to Semiconductor Heterostructures*, (Les Editions de Physique, Les Ulis, 1989).
[8] J. R. Guest *et al.*, Science 293, 2224 (2001).
[9] K. Matsuda, T. Saiki, S. Nomura, M. Mihara, and Y. Aoyagi, Appl. Phys. Lett. **81**, 2291 (2002).
[10] K. Matsuda, T. Saiki, S. Nomura, M. Mihara, and Y. Aoyagi, in *Physics of Semiconductors 2002*, Eds. A. R. Long and J. H. Davies (Inst. of Phys. Publ., Bristol, UK, 2002).
[11] K. Matsuda, T. Saiki, S. Nomura, M. Mihara, Y. Aoyagi, S. Nair, and T. Takagahara, Phys. Rev. Lett. **91**, 177401 (2003).
[12] R. Zimmermann, Pure and Applied Chemistry **69**, 1179

(1997).
[13] D. A. Kleinman, Phys. Rev. B **28**, 871 (1983).
[14] E. A. Hylleraas and A. Ore, Phys. Rev. **71**, 493 (1946).
[15] W. F. Brinkman, T. M. Rice, and B. Bell, Phys. Rev. B **8**, 1570 (1973).
[16] G. Pistone, S. Savasta, O. Di Stefano, and R. Girlanda, Phys. Rev. B **67**, 153305 (2003).
[17] O. Mauritz, G. Goldoni, F. Rossi, and E. Molinari, Phys. Rev. Lett. **82**, 847 (1999); Phys. Rev. B **62**, 8204 (2000).
[18] C. Simserides, U. Hohenester, G. Goldoni, and E. Molinari, Phys. Rev. B **62**, 13 657 (2000).
[19] U. Hohenester, G. Goldoni, and E. Molinari, unpublished.
[20] K. Matsuda, private communication.
[21] With the material parameters of Ref. 18 we find energies of −8.686, −8.442, −8.128, and −8.043 meV for the exciton groundstate and the first three excited exciton states, respectively, and −17.264 meV for the biexciton groundstate; exciton (biexciton) energy zero is given by the energy of the two-dimensional exciton (biexciton) of the narrow quantum well.[13] Note that we are not attempting a quantitative comparison of the total exciton and biexciton energies because of the well-known problems regarding the underestimation of the biexciton binding for the trial wavefunction under consideration; for a discussion see, e.g., O. Heller, Ph. Lelong, and G. Bastard, Phys. Rev. B **56**, 4702 (1997).